Impact of microcarrier concentration on mesenchymal stem cell growth and death: Experiments and modeling

Charlotte Maillot, Natalia De Isla, Celine Loubiere, Dominique Toye, Eric Olmos

Received: 13 May 2022 | Revised: 31 August 2022 | Accepted: 6 September 2022

DOI: 10.1002/bit.28228

ARTICLE

BIOTECHNOLOGY AND BIOENGINEERING WILEY

Impact of microcarrier concentration on mesenchymal stem cell growth and death: Experiments and modeling

Charlotte Maillot[1,2] | Natalia De Isla[3] | Celine Loubiere[1] | Dominique Toye[3] | Eric Olmos[1]

[1]Laboratoire Reactions et Genie des Procedes, Universite de Lorraine, CNRS UMR 7274, Nancy, France

[2]Department of Chemical Engineering, Product Environment and Processes (PEPs), Universite de Liege, Liege, Belgium

[3]Department of Chemical Engineering, Product Environment and Processes (PEPs), Universite de Liege, Liege, Belgium

Correspondence
Eric Olmos, Laboratoire Reactions et Genie des Procedes, Universite de Lorraine, CNRS UMR 7274, Nancy, France.
Email: eric.olmos@univ-lorraine.fr

Funding information
Université de Lorraine

Abstract

Mesenchymal stem cell (MSC) products are promising therapeutic candidates to treat a wide range of pathologies. The successful commercialization of these cell therapies will, however, depend on the development of reproducible cell production processes. For this, using microcarriers as growth supports within controlled conditions may be a viable process option. Although increasing microcarrier concentration may be associated with greater productivity due to the increased available culture surface, additional friction or shocks between microcarriers are likely to lead to undesired cell death. However, data detailing the impact of microcarrier collisions on MSC growth remains scarce. The following work demonstrates that MSC growth on microcarriers is greatly influenced by particle concentration even when little impact is observed on the apparent growth rate. It is suggested that the apparent growth rate may result in an equilibrium between growth and death kinetics which are independently affected by particle concentration and that certain MSC quality attributes may be progressively degraded in parallel. In addition, the theoretical reduction of the MSC growth rate was modeled according to the ratio between the average interparticle distance and the Kolmogorov scale. This study is an original contribution toward understanding the hydrodynamic effects in microcarrier-based stem cell cultures.

KEYWORDS
cell kinetics, hydrodynamics, mesenchymal stem cells, microcarriers

1 | INTRODUCTION

Since the beginning of the 21st century, the discovery and development of various advanced therapy medicinal products have triggered an increasing number of clinical trials using human cells. Carried by this movement, mesenchymal stem cells (MSCs) have been gradually used as cell therapies to address a wide range of pathologies including neurodegenerative or respiratory diseases (Rodriguez Fuentes et al., 2021; Trounson & McDonald, 2015), but also as raw materials for tissue reconstruction, for example, in view of grafting epithelial and skeletal assemblies (Bianco & Robey, 2001; Ringe et al., 2002). More recently, the discovery of therapeutic bioactive products secreted by MSCs has resulted in the development of processes for which the production of MSCs is no longer performed for the cells themselves but rather the molecules they produce (Riazifar et al., 2017). Regardless of how the cells are used, most therapeutic applications require around 1–1000 million cells per patient per dose (Chen et al., 2013; Rodriguez Fuentes et al., 2021), exceeding the amount of cells that can be extracted from a single donor. As a result, an ex vivo expansion phase is usually required, traditionally performed using monolayer or multilayer tissue flasks of different sizes (Ikebe & Suzuki, 2014). Although this method of

expansion is well documented in literature, it is labor intensive and introduces contamination risks due to the required manual cell passaging between different containers. In addition, controversies persist between research teams concerning optimal process parameters to use during the expansion process and their impact on the final cell product (Maillot et al., 2021). Various lead clinical trials using MSCs produced this way have either failed to meet the requirements for phase progression or undergone early termination (Parekkadan & Milwid, 2010), indicating that important bottlenecks still remain to successfully commercialize these therapies.

To scale up the manufacturing of high-quality stem cell products, a shift to three-dimensional (3D) cultures using bioreactors may be required (Godara et al., 2008; Hoch & Leach, 2014). For this, adherent MSCs are no longer cultured in planar conditions but using embryoid bodies (small aggregates of cells in suspension), microcapsules containing the cells, or microcarriers (small particles in suspension on which adherent stem cells expand). Using 3D culture brings flexibility to the process, enables high-density cell expansion in conditions that can easily be monitored, reduces the risk of contamination (McKee & Chaudhry, 2017), and significantly reduces the cost and space required for GMP manufacturing (Russell et al., 2018). However, to our knowledge, out of the 10,353 clinical trials involving MSCs in 2021, only two clinical studies have been completed using a bioreactor-based MSC expansion strategy (laryngotracheal engineered tissue transplantation NCT01997437 and placenta-derived mesenchymal-like stem cells expanded in PluriXTM 3D bioreactors for intramuscular injections NCT00919958). None of the clinical trials seem to involve a microcarrier-based approach, possibly indicating the need to continue fundamental research on these processes, in particular, to understand how both solid and liquid phases interact and impact MSC expansion.

In this mindset, optimizing microcarrier concentration may prove to be critical. While pioneering work using human fibroblasts showed no significant impact on increasing Sephadex (particle diameter ≈ 180 µm) microcarrier concentration from 5 to 15 g/L (Hu et al., 1985), successive studies showed that increasing Cytodex-1 (particle diameter ≈ 190 µm) microcarrier concentration above a threshold of approximately 1 g/L was associated with a decreased observed specific growth rate (Croughan et al., 1988). More recently, similar results have shown a deleterious effect of increasing microcarrier concentration from 3000 to 7500 Cytodex-3 microcarriers per mL (particle diameter ≈ 175 µm) during MSC growth (Hewitt et al., 2011) while other studies showed this negative impact of increasing Cytodex-3 microcarrier concentration only after a certain threshold of 8 g/L (Chen et al., 2015). Although a certain heterogeneity persists in literature, an overall consensus tends to show that increasing microcarrier concentration is, in general (and sometimes after a certain threshold), associated with a negative impact on growth.

In addition, cell damage typically may occur in agitated conditions due to (1) collisions between cells on microcarriers and the impeller or culture vessel, (2) collisions between microcarriers, and/or (3) interactions with turbulent flow eddies approximately the same size as the microcarriers on which cells are grown (Cherry & Papoutsakis, 1988). Consequently, the negative impact of microcarrier concentration on growth is often attributed to microcarrier–microcarrier interactions without, to our knowledge, a robust scientific demonstration for MSCs.

The aim of the present study is to provide a detailed description of the impact of microcarrier concentration on human MSC growth by testing a wider range of microcarrier concentrations (α), using microcarriers of different sizes, and through different agitation systems. Supplementary cultures to which various concentrations of plastic particles (β) were added also contributed to further describing the impact of repeated mechanical constraints on human MSC expansion dynamic parameters (Figure 1). Adding these plastic particles, on which cells cannot adhere and were found to not grow, provoked particle-microcarrier collisions without providingadditional cell culture surfaces. Combining both sets of experiments was then used to evaluate the theoretical real growth rate in each system. In addition, immmunophenotyping was performed on MSCs after their growth on microcarriers to define the potential impact of microcarrier concentration on cell phenotype.

2 | EXPERIMENTAL APPROACH

2.1 | Cell extraction, primary cultures, and cell culture medium

Human MSCs were extracted from the Wharton's Jelly of umbilical cords from just-born babies (Centre Hospitalier Universitaire de Nancy) and expanded and cryopreserved according to methods previously described (Martin, 2017; Reppel, 2014). A primary expansion was performed after thawing individual cryovessels onto standard T-Flasks for 5–10 days. At least two independent donor cell banks were used for each set of experiments. All cultures were performed in a CO_2 incubator (MCO 215LIT; Sanyo) (37°C, 5% CO_2) and α-MEM medium (11590606; Thermo Fisher Scientific) supplemented with 5% human platelet lysate (HPL) (BC0190020; Macopharma or PL-NH-500; Sexton Biotechnologies), 1% (vol/vol) antibiotic antimycotic solution (A5955; Sigma-Aldrich) and 4 mM glutamine (G7513; Sigma-Aldrich). In cultures performed using the HPL supplied by Macopharma, a mechanical defibrination of the medium was performed to limit the development of a gel-like matrix during agitated cultures (Laner-Plamberger et al., 2015), and primary cultures were performed with the addition of 2 IU/ml heparin (H3149; Sigma-Aldrich). For each set of experiments, the same HPL supplier was used throughout all cell culture stages.

2.2 | Microcarrier-based cultures protocols in Erlenmeyer flasks or spinner flasks

After having previously prepared either Cytodex-1 microcarriers (17044802; Cytiva Lifesciences) or Synthemax II Dissolvable microcarriers (7290; Corning) according to the manufacturer's instructions, hMSCs were inoculated for 4 h in either Erlenmeyer flasks (EF) (PVB125; Thermo Fisher Scientific) or spinner flasks (SF) (Schott

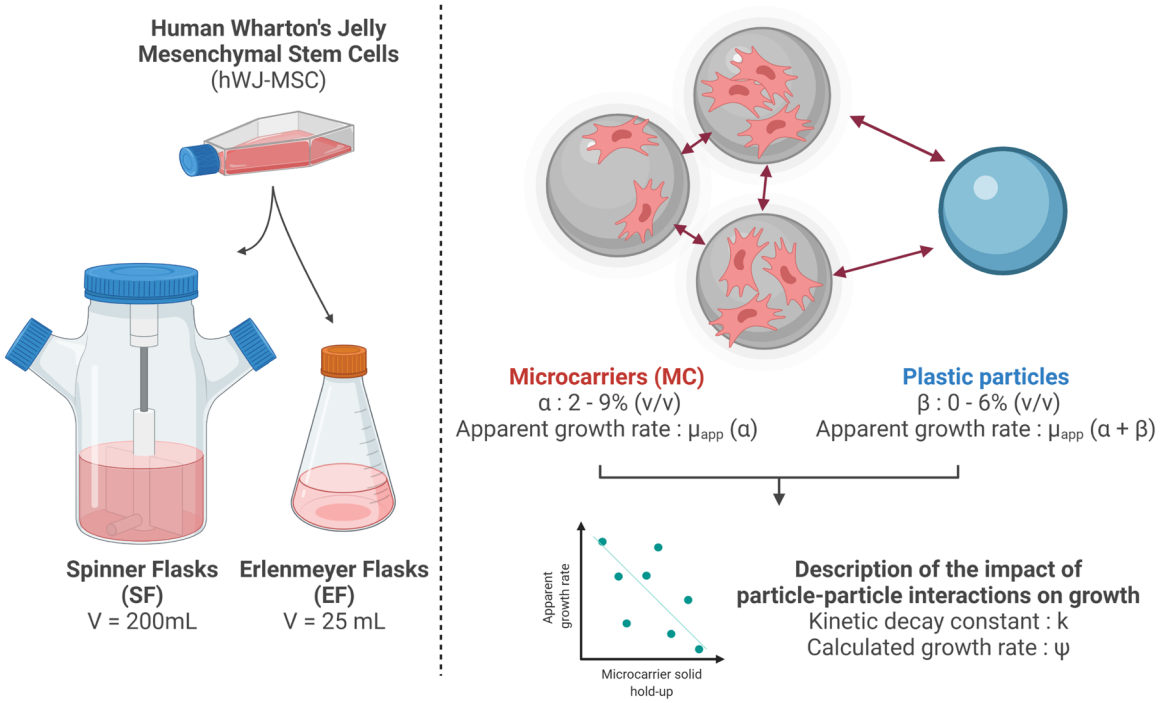

FIGURE 1 Experimental approach used to determine the impact of microcarrier interactions on human Wharton's jelly mesenchymal stem cell (hWJ-MSC) growth. MSCs were grown at various microcarrier concentrations (α) and with various added particle concentrations (β) in both spinner flasks (SF) and Erlenmeyer flasks (EF). The apparent growth rate in each condition could then be calculated (μ_{app}). Figure created with biorender.com

bottles agitated with Duran GL 45 stirred reactor agitators; Z680788-1KT; Merck) at an initial concentration of 7500 cells/cm^2 which was previously defined as optimal (Sion et al., 2020). The initial adhesion phase was performed without HPL in half of the final working volume and either in static conditions (EF) or using intermittent agitation cycles of 5 min every 30 min for 2 h followed by cycles of 5 min every 60 min for 2 h (SF). These conditions were found to increase the initial attachment yield compared to a 4 h static adhesion phase in a medium containing HPL. After cell adhesion, the medium was completed to the final volume and HPL was added. Half of the culture supernatant was replaced every 3–4 days by a fresh medium to limit the accumulation of by-products and feed the cell culture.

A range of microcarrier concentrations were used for cell culture (4.4%–9.0% [vol/vol] (EF) or 2.7%–6.6% [vol/vol] (SF)). In certain experiments, a constant microcarrier concentration was used (4.4% [vol/vol] (EF) or 2.7% [vol/vol] (SF)) to which a range of plastic particles (P102-1521; Pall SoloHill) was added on which cell growth was not observed and has been shown to be negligible (Loubière et al., 2019). These particles have a similar size and density as the microcarriers used for cell growth and, as a result, provoke additional collision forces during cell culture without increasing the available cell culture surface. The microcarrier concentrations in SF and EF in the control conditions were chosen as have previously been shown to successfully support cell growth in these agitation systems (Sion et al., 2020). Agitation conditions were fixed at the particle just suspended state $N = N_{js} \approx 70$ rpm (EF) or $N = N_{js} = 40$ rpm (SF). We can note that the impact of particle concentration on the agitation rate required to maintain particles in suspension was found to be negligible for the particle concentrations used, according to the well-known Zwietering equation (Zwietering, 1958). The complete suspension of particles in each condition was also visually verified.

2.3 | Characterization of kinetic parameters during MSC cell expansion on microcarriers

2.3.1 | Cell growth characterization

Cell counting of the total amount of live cells on microcarriers X was performed at least daily in all experiments by analyzing a homogeneous 500 µL sample of the cell culture. For Cytodex-1 experiments, attached cells were counted by automatic recognition of fluorescent nuclei attached to microcarriers after DAPI–methanol staining. By using methods previously described, the average number of cells per microcarrier can be obtained from at least six different microscopic observations (Loubière et al., 2019). Cells counted directly on the microcarriers were presumed to be live cells. For Synthemax II experiments, microcarriers were left to sediment and the pellet was dissolved by using a trypsin–pectinase solution according to the manufacturer's recommendations. After dissolution, the cell suspension solution was filtered (100 µm mesh) and counted using an automatic cell counter (Vi-Cell XR; Beckman Coulter). Regardless of the microcarrier type, only the cells which were attached to the microcarriers were counted.

The theoretical initial viable cell concentration attached to microcarriers X_i was calculated by multiplying the amount of cells initially seeded by the average inoculation yield in each system. This value was preferred over the measured initial cell concentration to smooth the impact of counting variability which can be imprecise at the beginning of the cell culture due to low initial cell concentrations, and an inoculation yield which could also be variable between conditions. Subsequently, the apparent growth rate μ_{app} was determined by fitting Equation (1) to the experimental data points during the exponential growth phase.

$$X(t) = X_i \times e^{\mu_{app} \times t} \quad (1)$$

The apparent MSC growth rate was determined at various microcarrier concentrations α. For each microcarrier concentration, experiments were performed in duplicate or triplicate analysis. Theoretically, the apparent growth rate at a given microcarrier concentration $\mu_{app}(\alpha)$ is affected by both cell growth and death kinetic decay constants. Accordingly, MSCs would theoretically have a growth rate $\Psi(\alpha)$ if microcarrier–microcarrier interactions were absent and did not cause additional mortality. We should note that in all experiments, a constant seeding cell density was applied of 7500 cells/cm^2. As a result, increasing microcarrier concentration and cell culture surface also induces higher volumetric cell concentrations throughout the cell cultures. It is supposed that the theoretical growth rate $\Psi(\alpha)$ may be dependent on microcarrier concentration due to different levels of secreted growth factors or toxic metabolic by-products which can enhance or inhibit growth (Croughan et al., 1988).

In addition, the negative impact of particle-particle interactions on cell growth is presumed to follow a first-order kinetic model according to microcarrier concentration α (Croughan et al., 1988). As a result, performing experiments at various microcarrier concentrations gives important information on how growth is impacted and can be modeled by Equation (2). However, these experiments alone are not sufficient to determine the kinetic decay constant k nor the MSC growth rate in the system which would occur without microcarrier-microcarrier interactions $\Psi(\alpha)$.

$$\mu_{app}(\alpha) = \Psi(\alpha) - k \times \alpha \quad (2)$$

To obtain the kinetic decay constant k, a separate set of experiments was performed by adding plastic particles after the initial cell attachment phase, on which cells did not attach nor grow. These plastic particles were added at various concentrations β while the microcarrier concentration α was kept constant. It is noteworthy that although it has been observed that cells grow on plastic microcarriers (with very low growth and attachment rates, Loubière et al., 2019), this was not found to be the case in the concomitant presence of Cytodex-1 or Synthemax II microcarriers. Daily DAPI staining of cells in all of the Cytodex-1 experiments showed no attachment or growth on these particles which were therefore considered as not providing additional adherence surfaces.

For each microcarrier concentration, experiments were performed in duplicate or triplicate analysis except for experiments performed using Synthemax II microcarriers in EF. For this last experiment, the experimental error was estimated based on the mean experimental variability measured in EF and Cytodex-1 microcarriers. Subsequently, Equation (2) was used to describe the apparent growth rate $\mu_{app}(\alpha + \beta)$ according to both growth and death constants. First, the theoretical growth rate which would occur in the system if microcarrier–microcarrier interactions were absent $\Psi(\alpha)$ is considered constant in these set of experiments since the microcarrier concentration is not modified and growth on the plastic microcarriers is absent (i.e., $\Psi(\alpha + \beta) \approx \Psi(\alpha)$). Second, this growth rate should be reduced by microcarrier–microcarrier interactions according to a first-order kinetic model represented by the constant k. Finally, the impact of particle-microcarrier interactions can be supposed as having a kinetic decay constant of $k/2$ since, on average, a microcarrier containing cells meets a plastic particle twice less frequently since only half of the interacting particles have cells. Solving Equation (3) with various particle concentrations β allowed us to determine two critical system constants: the MSC growth rate which would occur without microcarrier interactions at the control microcarrier concentration $\Psi(\alpha)$; and the kinetic decay constant due to microcarrier and particle interactions k.

$$\mu_{app}(\alpha + \beta/2) = \Psi(\alpha) - k \times \left(\alpha + \frac{\beta}{2}\right) \quad (3)$$

Finally, combining the results obtained at various microcarrier concentrations and the results obtained with the addition of plastic particles allowed us to solve Equation (2) after having determined k with Equation (3). These results shed new light on how the growth rate in microcarrier-based cell culture systems is impacted by microcarrier concentration.

2.3.2 | Metabolite analysis

Glucose and lactate concentrations were measured daily using an offline analyzer (Gallery multi-parametric analyzer; Thermo Fisher Scientific) and used to calculate the specific glucose consumption rates $q_{Gluc/X}$ and specific lactate production rates $q_{Lac/X}$ over the exponential growth phase $\Delta t_{i->f}$ (Equations 4 and 5). For this, the initial i and final f metabolite concentrations were used as well as the variation in metabolite concentration during medium changes $\Delta Gluc$ or ΔLac. Lastly, the transformation yield of glucose to lactate during the exponential phase was calculated (Equation 6). Considering the low volumes of experiments in EF and detachment yields on Cytodex-1 microcarriers, this analysis was limited to SF experiments using Synthemax II microcarriers.

$$q_{Gluc/X} = \frac{Gluc_i - Gluc_f + \Delta Gluc}{X_f - X_i} \times \frac{1}{\Delta t_{i->f}} \quad (4)$$

$$q_{Lac/X} = \frac{Lac_f - Lac_i + \Delta Lac}{X_f - X_i} \times \frac{1}{\Delta t_{i->f}} \quad (5)$$

$$Y_{Lac/Gluc} = \frac{q_{Lac/X}}{q_{Gluc/X}} \quad (6)$$

2.3.3 | Immunophenotyping

MSCs expanded on Synthemax II microcarriers in SF were detached at the end of the exponential growth phase and cryopreserved at a concentration of 5×10^6 cells/ml. These cells were then thawed and cultured for 3 days before characterization according to the general guidelines provided by the International Society for Cellular Therapy (ISCT) (Dominici et al., 2006). Plastic adhesion was verified at this stage. For flow cytometry, approximately 1×10^5 cells were resuspended in 100 µL phosphate buffer saline (PBS) supplemented with bovine serum albumin and incubated with specific antibodies for 1 h at room temperature. After incubation, MSCs were washed with PBS, centrifuged at 300 g for 5 min, and resuspended in 250 µL of 1% paraformaldehyde until analysis by FACS flow cytometry (Gallios; Beckman Coulter) according to methods and specific antibodies previously described (Sion et al., 2021).

2.3.4 | Cell death characterization

To further characterize live and dead cell populations at the end of the cell culture, a detailed analysis was performed on cells that were grown in SF on Synthemax II microcarriers. These conditions were chosen since the larger volume of the SF allowed a greater sampling capacity and since cells grown on Synthemax II were shown to have the greatest cell detachment yield. Live and dead cells attached to the Synthemax II microcarriers were quantified after microcarrier dissolution using an offline cell analyzer (Vi-Cell; Beckman Coulter). This quantification was performed on three independent 500 µL homogeneous samples. In addition, cell lysis was quantified through supernatant lactate dehydrogenase (LDH) concentration which was measured at the start and end of the cell culture using an offline analyzer (Gallery multi-parametric analyzer; Thermo Fisher Scientific). This technique was calibrated by measuring the LDH concentration before and after four freeze-thaw cycles of five MSC cell dilutions. Measuring cell concentration after these cycles showed no more live cells, indicating all cells had undergone lysis during these cycles. The conversion factor of 1 IU LDH to 2.1×10^6 lysed cells was used to determine cell death during the cell culture.

3 | RESULTS AND DISCUSSIONS

3.1 | Impact of microcarrier concentration on cell growth kinetics

3.1.1 | Observed cell growth during microcarrier-based cell culture

The first set of experiments were performed at various Cytodex-1 and Synthemax II microcarrier concentrations using both EF and SF. To begin with, the impact of microcarrier concentration on the capacity of cells to effectively colonize each microcarrier surface was evaluated. For this, the maximum cell concentration was measured at the end of the exponential growth phase (Figure 2, left). As a reference, the initial seeding cell concentration in all conditions was 7500 cells/cm^2. This would be the initial cell concentration if the attachment yield was 100%. The measured average inoculation yields in each condition are also presented in Appendix S1. It can be noted that, in general, seeding was found to be more efficient in SF due to the greater volume and more reproducible agitation conditions during

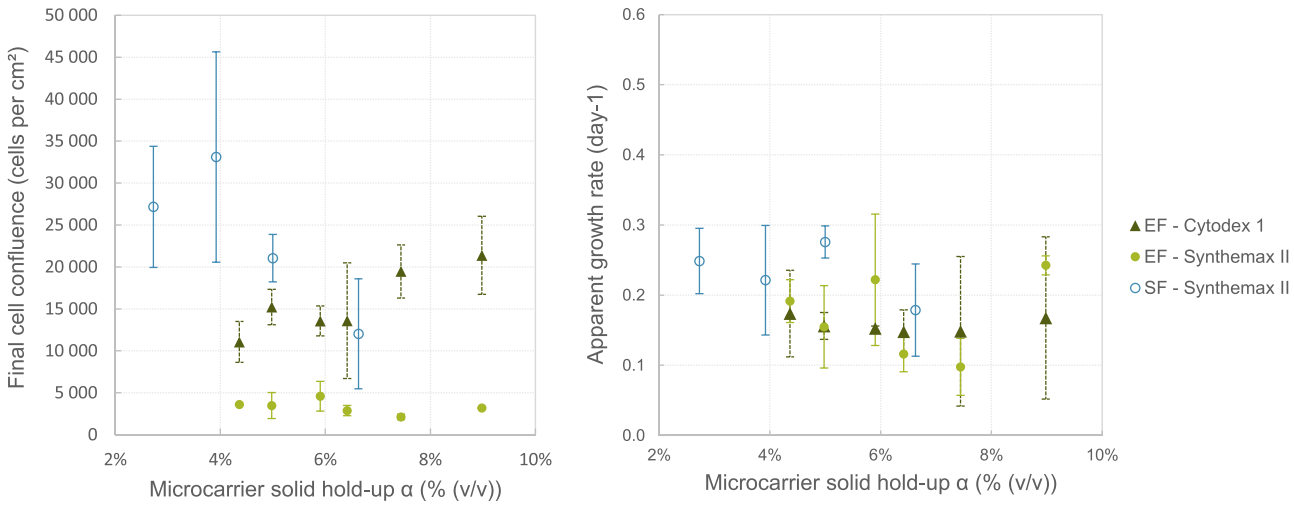

FIGURE 2 Left: Maximum cell surface concentration observed at the end of the exponential growth phase of hWJ-MSCs grown on either Cytodex-1 or Synthemax II in either spinner flasks (SF) or Erlenmeyer flasks (EF) at various solid hold-up concentrations (α). Right: Apparent growth rate ($\mu_{app}(\alpha)$) measured at various microcarrier solid hold-up concentrations (α). Error bars correspond to the standard deviation measured between different cultures performed in duplicate or triplicate analysis.

the initial attachment phase. Finally, no significant trends were observed in the seeding efficiency when increasing particle concentration.

In SF using Synthemax II microcarriers, similar levels of confluence were observed at the end of the exponential growth phase for cell cultures performed between 2.7% (vol/vol) and 5% (vol/vol) (for comparison, the average length of the exponential growth phases observed in these conditions can be found in Table 1). However, increasing microcarrier concentration past 5% (vol/vol) was found to reduce microcarrier colonization. These results indicate that certain factors in high microcarrier concentrations (possibly microcarrier–microcarrier interactions) may be limiting cells from achieving confluence through either increased cell death or mechanical factors which cause cells to detach from microcarriers. In the case of EF, however, little impact of microcarrier concentration on cell colonization was observed in both Cytodex-1 and Synthemax II microcarrier cell cultures, indicating that cells are reaching similar confluence levels in all conditions regardless of microcarrier concentration. Notably, the final cell surface concentration was found to be lower than the theoretical initial seeded cell concentration when using Synthemax II microcarriers. This may be caused by the fact that the inoculation yield was lower in these conditions (only approximately 20% of the inoculated cells adhered to the microcarriers).

In addition, the speed at which cells reached confluence was obtained by fitting experimental data to known growth models. No notable impact of microcarrier concentration on the observed growth rate was observed in EF or SF and regardless of the microcarrier used (Figure 2, right). In all of the conditions observed, the apparent growth rate $\mu_{app}(\alpha)$ remained within typical process variability (obtained by calculating the standard deviation of the results obtained in duplicate or triplicate analysis).

To further understand how microcarrier–microcarrier interactions affect MSC growth when increasing microcarrier concentration, separate experiments were performed with a constant concentration of either Cytodex-1 or Synthemax II microcarriers in SF (2.7% [vol/vol]) and EF (4.4% [vol/vol]). These concentrations were chosen since the growth of WJ-MSCs has previously been demonstrated as successful in both agitation systems in these conditions (Sion et al., 2020). Plastic particles were added at various concentrations (β) after the initial attachment phase. Cell growth was not observed on the added plastic particles.

To begin with, analysis of growth data seemed to indicate that cells grown with added plastic particles had a slower apparent growth rate and that the effect was increased the more plastic particles were added. For instance, the growth kinetics of 3 conditions among 12 and modeled growth curves can be observed in Figure 3, left, and indicates this trend. Notably, in cases where high particle

TABLE 1 Average exponential growth phase duration for experiments presented in Figure 2.

Exponential growth phase duration (in days)						
Total solid hold-up (%v/v)	**4.4**	**5.0**	**5.9**	**6.4**	**7.4**	**9.0**
EF—Cytodex-1	2.8	4.4	4.2	4.9	9.0	7.8
EF—Synthemax II	7.5	8.1	7.5	7.5	6.9	7.3
Total solid hold-up (%vol/vol)	**2.7**	**3.9**	**5.0**	**6.6**		
SF—Synthemax II	7.0	7.9	6.5	6.8		

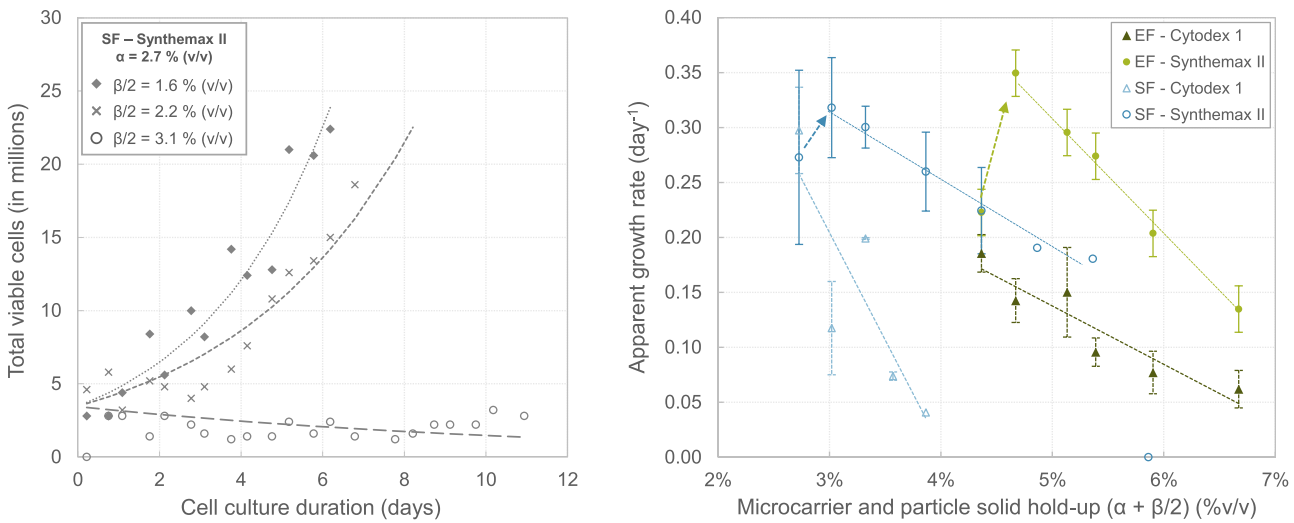

FIGURE 3 Left: MSC cell growth on Synthemax II microcarriers (MC) (α = 2.7% [vol/vol]) in spinner flaks (SF) with the addition of plastic particles ($\beta/2$). Right: Apparent MSC growth rate for constant Cytodex-1 or Synthemax II concentrations (α) and various concentrations of plastic particles ($\beta/2$) in Erlenmeyer flasks (EF) and spinner flasks (SF). Error bars correspond to the standard deviation measured between different cultures performed in duplicate or triplicate analysis except for experiments performed using Synthemax II microcarriers in Erlenmeyer flasks. For this last experiment, the experimental error was estimated based on the mean experimental variability measured in Erlenmeyer flasks and Cytodex-1 microcarriers.

concentrations were added ($\beta/2 > 3\%$ [vol/vol]), the apparent growth rate was negative, indicating a higher death rate than the real growth rate. Fitting exponential growth models to the experimental data observed was then used to determine the apparent growth rate at various plastic particle concentrations and using both Cytodex-1 and Synthemax II microcarriers. Regardless of the agitation system or the microcarrier used, a linear decrease in the MSC apparent growth rate was observed when increasing the total particle concentration (Figure 3, right). Similar results have previously been observed for human FS-4 fibroblast growth on Cytodex-1 microcarriers (Croughan et al., 1988) to which various concentrations of particles were added. Similarly to the hypothesis proposed, the decrease in the MSC growth rate observed may be caused by repeated mechanical constraints caused by the additional particles added, as it has been shown that frequent mechanical stresses suppress the proliferation of human MSCs (Frank et al., 2016).

These linear fitting of these experimental results was then used to identify the kinetic decay constant k caused by microcarrier–particle interactions using Equation (3) for each agitation system (Table 2). Interestingly, this constant was found to depend on the microcarrier type used, possibly due to the different physical characteristics of each microcarrier. To begin with, microcarrier size typically impacts the frequency and force which occur during the collisions between two particles. For the same solid hold-up, smaller particles will have a higher collision frequency but of lower intensity. In addition, the difference in material surface elasticity impacts how the collision force will be transmitted to the cell as an elastic surface may absorb part of the collision force (Cherry & Papoutsakis, 1986). In addition, the choice of an agitation system was also found to have an impact on how these added particles impact cell growth. As a result, it is possible that for a given solid hold-up, different mechanisms exist in either SF or EF, possibly due to differences in the spatial distribution of microcarriers caused by the agitation system. The use of an external agitation method in EF typically concentrates particles in the middle of the flask which may lead to an increased frequency of collisions and/or friction between particles in these systems and thus affect cell growth in a different manner than in cell cultures for which microcarriers are suspended using an impeller (Öncül, 2010). Interestingly, the impact of adding plastic particles was found to be most significant in EF using Synthemax II microcarriers and in SF using Cytodex-1 microcarriers which may seem to indicate that both the agitation system (ie. particle suspension and homogeneity) and the type of microcarrier used (ie., size and elasticity) affect the way these microcarrier interactions affect cell growth.

In addition, fitting the observed growth rate with Equation (3) was then used to determine the growth rate of the control condition which would theoretically be obtained if particle-particle interactions were absent $\Psi(\alpha)$. This growth rate can then be compared to the apparent growth rate in the control condition $\mu_{app}(\alpha)$. Results indicate, in all conditions, that the measured growth rate in the system may largely underestimate the growth rate without these added mechanical constraints. These results may indicate that growing cells under different mechanical constraints may also have an impact on the quality of the cells obtained at the end of the cell culture (cells may be undergoing more divisions than measured or have altered phenotypical characteristics and as a result may be reaching senescent states earlier than they would in static conditions).

Finally, interesting results were observed for cells grown on Synthemax II microcarriers in both Erlenmeyer and SF. In these cases, adding small amounts of plastic microcarriers to the cell culture was found to have a beneficial impact on the apparent growth rate as represented by the arrows in Figure 3. As a result, the linear fitting was performed by excluding the results obtained in the control conditions for a more accurate calculation of the mechanical decay kinetic constant in these conditions. The increase in the apparent growth rate in these conditions may be explained by a reduced aggregation between cells and microcarriers since the plastics particles may break these cell-microcarrier aggregates and create greater homogeneity in the systems but additional experiments should be performed in this range of plastic particle concentration to confirm the possible positive effect at very small concentrations.

3.1.2 | Observed cell death at the end of microcarrier cell culture

As suggested above, increasing particle concentration during MSC cell culture on microcarriers seems to have a significant impact on cell growth. Notably, the apparent cell growth rate was found to decrease with increasing added plastic particle concentration. To determine if this decreased apparent growth rate was due to overall slower cell growth, or due to an increased amount of cell death in the system, the quantity of live and dead cells at the end of MSC cell cultures grown on Synthemax II microcarriers was measured in SF (Figure 4). These conditions were chosen since they provided the greatest sampling capacity and since cells were most easily detached from the microcarriers for analysis.

TABLE 2 Growth kinetic parameters calculated for MSC cultures grown on Synthemax II and Cytodex-1 microcarriers in Erlenmeyer flasks (EF) and spinner flasks (SF).

Culture system (microcarrier)	Control apparent growth rate, $\mu_{app}(\alpha)$ (day^{-1})	Control growth rate without mechanical constraints, $\Psi(\alpha)$ (day^{-1})	Kinetic decay constant, k (day^{-1})
EF (Cytodex-1)	0.19	0.40	5.3
EF (Synthemax II)	0.22	0.85	10.9
SF (Cytodex-1)	0.30	0.79	19.6
SF (Synthemax II)	0.27	0.61	9.3

To begin with, the amount of live cells at the end of the cell culture was found to slightly increase with increasing microcarrier concentration or when increasing the amount of plastic particles added until a threshold of approximately 4% (vol/vol) in both cases. Afterward, the amount of live cells decreased when increasing microcarrier concentration. These results are similar to results previously obtained concerning human fibroblast cell growth on Cytodex-1 microcarriers and may indicate that deleterious effects of particle concentration may only impact microcarrier confluence after a certain threshold. Determining the cell viability in the system showed that, apart from extremely high particle concentrations of about 5.9%, viability at the end of the cell culture remained stable around approximately 50%–60% which seems to indicate that the decreased growth rate observed above should be correlated with a slower cell growth rather than an increased cell death.

In addition metabolic data were analyzed for cell cultures performed in SF with Synthemax II microcarriers. Glucose plays a central role in MSC cell metabolism as it is the primary energy source used through either oxidative phosphorylation or glycolysis. In all experiments, the average transformation yield from glucose to lactate was found to stay stable around 2 mol/mol indicating a preferential glycolysis metabolism in all cell cultures. Furthermore, in experiments with added plastic particles, the average glucose consumption rate and lactate production rate was also found to stay stable regardless of the particle concentration added (Figure 5, right). These results indicate that cells have, on average, similar metabolic activities since similar quantities of glucose were consumed per cell per day on average during the exponential growth phase. Finally, in experiments performed at various Synthemax II microcarrier concentrations, a slight increase in metabolic activity was found when increasing microcarrier concentration which may indicate that certain secondary metabolic pathways may be activated when increasing microcarrier concentration. Notably, it may be possible that cells respond to stresses identified by membrane mechanosensors by activating internal contractile or tension forces through, for example, myosin motors coupled with receptor-associated actin filaments (Romani et al., 2021). Due to the experimental restrictions presented above, the results of Figure 2 were

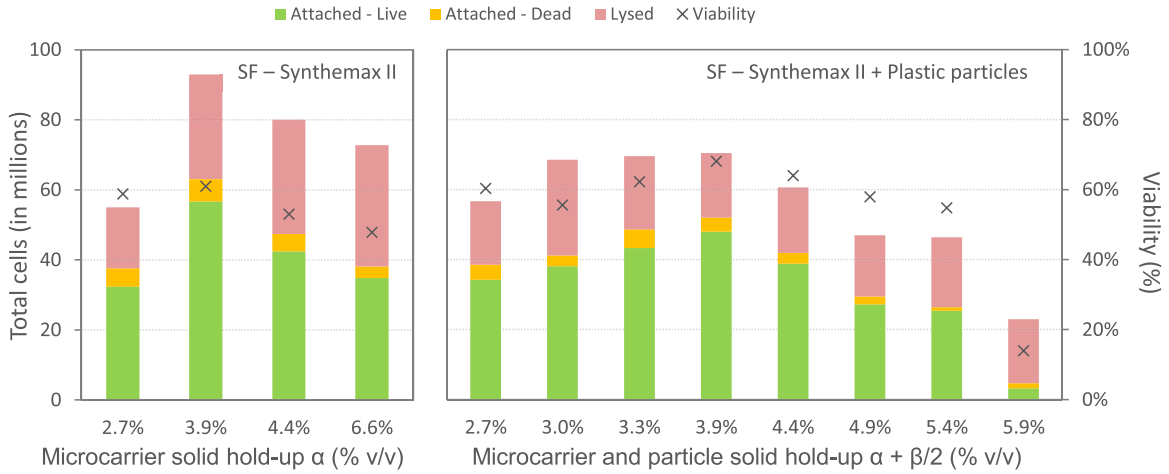

FIGURE 4 Live and dead cell populations counted at the end of the exponential growth phase of MSC cell cultures grown on Synthemax II microcarriers in spinner flasks (SF). Left: cells were grown at various microcarrier concentrations (α). Right: Cells were grown at a constant microcarrier concentration (α = 2.7% [vol/vol]) to which plastic particles were added (β).

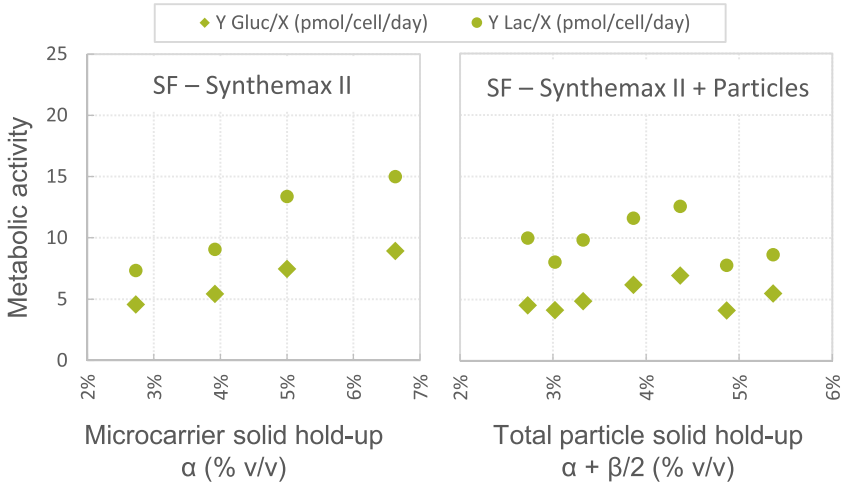

FIGURE 5 Kinetic metabolic parameters during MSC exponential growth at various Synthemax II MC concentrations in spinner flasks (SF). Cells were either grown at various MC concentrations (α) (left) or at a fixed MC concentration (α) with the addition of plastic particles at various concentrations β (right).

restricted to Spinner cultures with Synthemax II microcarriers. These results provide indications of possible general trends, but additional experiments would be necessary to confirm them.

3.1.3 | Immunophenotyping

Immunophenotyping results tend to indicate a progressive degradation of MSC cell marker expression with a significant impact at high microcarrier concentrations (>5% [vol/vol]) for which the criteria proposed by the ISCT (>95%) are no longer verified for CD44 and CD73 markers which have been reported to be associated with cell proliferation and MSC homing (Figure 6). We should note, however, that the expression of these cell markers remains high (>90%) and that all other cell markers showed no sign of degradation. In addition, significant overexpression of the CD106 marker has been observed for cells cultivated with increasing mechanical constraints through the addition of plastic particles during cell culture possibly indicating a progressive cell engagement towards certain vascular lineages as well as a slight underexpression of CD44, CD73, and CD166 surface markers. These results indicate the degradation of MSCs when grown under high mechanical stress conditions through increasing particle concentration, particularly at high microcarrier concentrations (>5% [vol/vol]).

3.1.4 | Calculated real cell growth rates during microcarrier-based cell culture

The evidence above seems to indicate that there may be fundamental underlying variations at stake when increasing microcarrier concentration in agitated conditions, even when no significant variation is observed when looking at the apparent growth rate in these cultures (Figure 2). To begin with, the kinetic decay constants due to microcarrier–microcarrier concentration were used to gain additional information on the theoretical growth rate which could occur without mechanical constraints in the cultures for which only the apparent growth rate could be observed (Figure 7). A theoretical growth rate much higher than the observed growth rate was found in experiments performed in EF using Synthemax II microcarriers for which the real growth rate was estimated as high as 1.2 day^{-1} in high microcarrier concentrations. These results indicate that the increased mechanical constraints in these conditions affect cell growth and, combined with metabolic data, may indicate that a higher metabolic activity per cell is required for cell maintenance.

3.1.5 | Modeling growth according to hydromechanical parameters

As suggested previously in extensive work performed on FS-4 cells grown on microcarriers, microcarrier collisions may arise through the action of turbulence in the fluid, and cell damage primarily occurs when the size of these turbulent eddies are comparable or smaller than the spacing between microcarriers (Croughan, 1988). In this mindset, the average interparticle distance in each system h was calculated according to Equation (7) (presuming particles are spherical with mean Sauter diameter D_{32}, homogeneously organized, and arranged in space in cubic order). This distance depends on the microcarrier and particle concentrations in each system as well as the packing limit α_m when particle distance reached 0 which was considered 52% (Mishra et al., 2014).

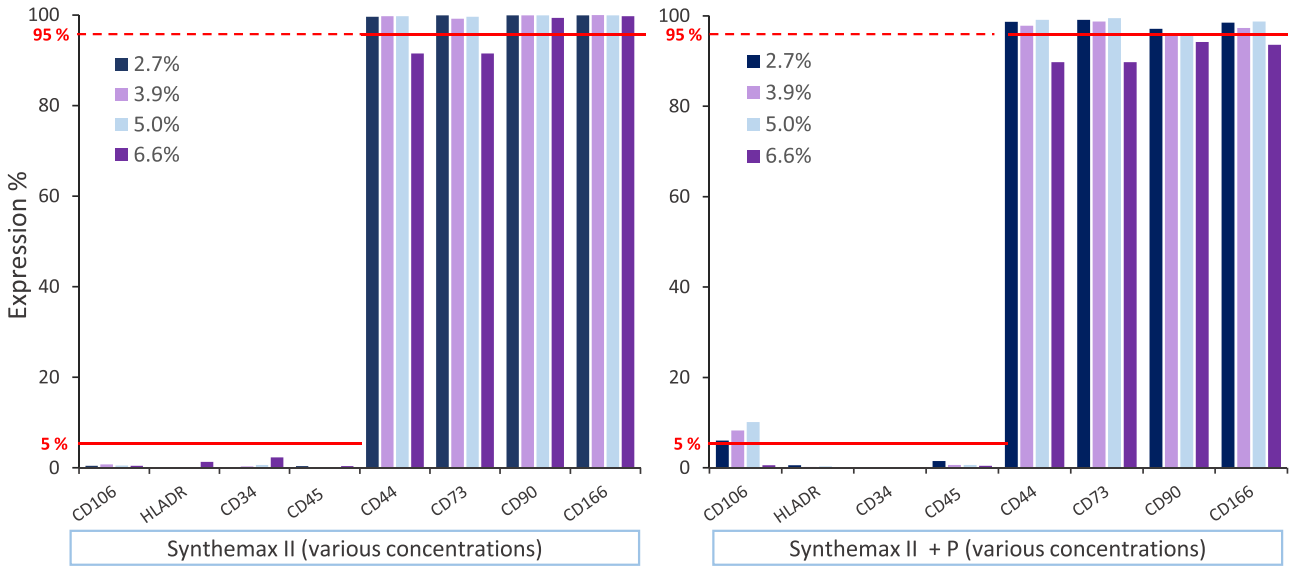

FIGURE 6 Percentage of cells expressing surface markers after expansion with various solid hold-up concentrations of Synthemax II microcarriers (left) or Synthemax II microcarriers and plastic particles (α + β).

$$h = D_{32}\left[\left(\frac{\alpha_m}{\alpha}\right)^{1/3} - 1\right] \quad (7)$$

Finally, the average Kolmogorov microscale of turbulence λ_k was calculated for each system and particle concentrations according to the method described in Appendix S2 using an approach previously described (Sion et al., 2020). As previously described in the literature, the impact of microcarrier interactions on cell growth typically begins to have an effect when the average distance between particles h is smaller than the size average smallest turbulent eddies in the system λ_k (Croughan et al., 1988). Since previous results indicate that a linear decrease in growth rate is observed when increasing microcarrier solid hold-up (Croughan, 1988), we propose a linear model based on a volumetric approach to this ratio h/λ_k, a constant representing collisions within each experimental setup $k_{\text{collision}}$ and the minimal theoretical growth rate which could be observed when the particle concentration reaches the packing limit $\mu_{\text{app}_{\text{lim}}}$ (Equation 8). Consequently, the theoretical reduction in growth rate caused by microcarrier–microcarrier interactions may be theoretically calculated for a given microcarrier concentration if the microcarrier size distribution and the agitation system chosen are sufficiently characterized.

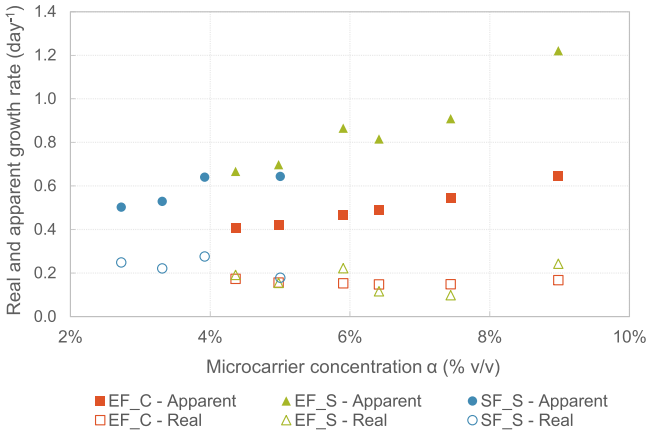

FIGURE 7 Apparent and calculated MSC growth rate at various microcarrier concentrations α in Erlenmeyer flasks (EF) or spinner flasks (SF) and with either Cytodex-1 (C) or Synthemax II (S) microcarriers.

$$\mu_{\text{app}}(\alpha) = k_{\text{collision}} \times \left(\frac{h}{\lambda_k}\right)^3 + \mu_{\text{app}_{\text{lim}}} \quad (8)$$

The data obtained with the addition of plastic particles is presented in Figure 8, left. A linear decrease in the standardized growth rate is observed when decreasing this ratio, and therefore when the interparticle distance becomes closer to the size of the smallest turbulent eddies in the system. The model proposed (Equation 8) can be used to predict the MSC growth rate reduction (Figure 8, right; Table 3) and represents, to our knowledge, the first results predicting MSC growth rate reduction on microcarriers using a model based on the physical characteristics of the cell culture system.

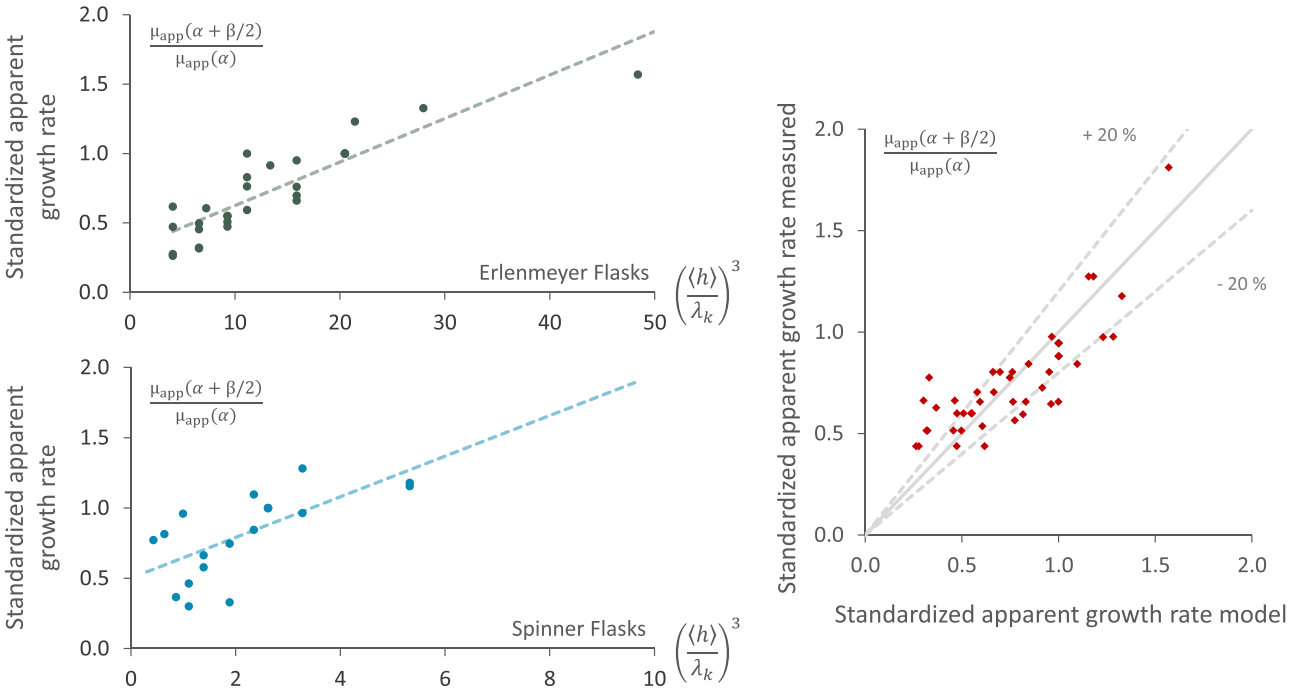

FIGURE 8 Apparent cell growth rate observed on Synthemax II and Cytodex-1 microcarriers in Erlenmeyer flasks (EF) (α = 4.4% [vol/vol]) or spinner flasks (SF) (α = 2.7% [vol/vol]) and added plastic particles (β) (left). Results are presented according to the average distance between particles calculated in each condition normalized to the average Kolmogorov turbulence microscale in each individual system. Linear fitting was then performed on the experimental data (right).

TABLE 3 Model parameters calculated to determine the impact of microcarrier–microcarrier interactions at various particle concentrations.

Culture system	Collision constant, $k_{collision}$	Theoretical standardized growth rate when at packing limit, $\mu_{app_{lim}}$
Erlenmeyer flasks	0.03	0.31
Spinner flasks	0.14	0.50

These results suggest that, in each geometrical setup, the decreased growth rate due to particle interactions will depend on the limit theoretical growth rate obtained when the particle concentration reaches the packing limit $\mu_{app_{lim}}$ and a constant representing these collisions within this experimental setup $k_{collision}$.

4 | CONCLUSION

MSC cell culture on microcarriers performed with increasing quantities of plastic particles brought to light the fact that increasing the total particle concentration seemed to have a negative impact on growth. Results obtained with MSCs were found to be similar to previous studies performed with human fibroblasts grown on microcarriers with the addition of other particles. A linear relationship seems to exist between the observed apparent growth rate and the quantity of added particles (Croughan et al., 1988). Data concerning LDH secreted in the media throughout the exponential growth phase was used to notice that cell death was not significantly upregulated to account for the decreased apparent growth rate. As a result, the most likely hypothesis may be that MSC mechanosensors can detect the increased mechanical constraints in these conditions (due to the added repeated friction and shocks caused by the added particles). Consequently, secondary metabolic pathways may be activated in response (thoroughly reviewed in Vining & Mooney, 2017). For example, myosin motors can be activated to increase cell rigidity and counter these mechanical constraints (Romani et al., 2021). Cells may also be undergoing morphological changes to adapt to the environment generated with repeated mechanical stresses as it has been shown that the hydromechanical environment (e.g., such as extracellular matrix rigidity) maintains stem and progenitor cell pools in adult epidermal niches (Zhu et al., 1999), or on the contrary, induces differentiation (Engler et al., 2006; Huebsch et al., 2010). Results indicating that similar levels of glucose were consumed per cell per day for a slower apparent growth seem to corroborate these results: the slower apparent cell growth indicates cells are dividing less fast and is associated with gradual changes in secondary metabolisms. Notably, cells maintained high levels of MSC surface marker expression. However, progressive degradation of CD44 and CD73 expression was observed in cultures performed with high particle concentrations. In addition, experiments performed with microcarriers of different sizes and rigidities, as well as different cell culture volumes and agitation systems seem to indicate that the impact of these mechanical constraints depends on these characteristics.

In parallel, experiments were performed at various microcarrier concentrations. In these experiments, little impact of the particle concentration was observed on the MSC apparent growth rate. However, the information obtained above indicates that underlying cell mechanotransduction signals are possibly taking place with increasing particle concentration without being identifiable by simply observing the apparent growth rate. As a result, the theoretical real growth rate in the system is possibly significantly higher than observed. In addition, gradual degradation of the MSCs produced was observed, as well as a gradual increase in cell senescence and replicative inhibition (data not shown) even if the MSCs produced met the common MSC criterion suggested by the ISCT (Dominici et al., 2006).

Finally, we present the first steps towards modeling and predicting growth reduction based on known physical properties of the cell cultures. Previous authors suggest that the increased death rate due to microcarrier interactions typically begins to have an effect when the average distance between particles h is smaller than the size average smallest turbulent eddies in the system λ_k (Croughan et al., 1988). The model we propose therefore takes into account the ratio between these physical characteristics and quite accurately allows us to predict the growth rate reduction based on these ratios.

AUTHOR CONTRIBUTIONS

Charlotte Maillot performed the experiments and wrote the original draft and figures. Celine Loubiere performed the CFD calculations and reviewed the manuscript. Dominque Toye, Natalia de Isla, and Eric Olmos supervised all aspects of the study and reviewed the manuscript. All authors contributed to the article and approved the submitted version.

ACKNOWLEDGMENTS

The authors would like to thank Caroline Sion, Naceur Charif, Amandine May, and Mégane Jeannelle for their valuable technical support. This study was supported by Lorraine University of Excellence/PhD grant 2019/R01PJZHX.

CONFLICT OF INTEREST

The authors declare no conflict of interest.

DATA AVAILABILITY STATEMENT

The data that support the findings of this study are available from the corresponding author upon reasonable request.

ORCID

Eric Olmos http://orcid.org/0000-0001-9063-0855

REFERENCES

Bianco, P., & Robey, P. G. (2001). Stem cells in tissue engineering. *Nature*, *414*(6859), 118–121.

Chen, A. K.-L., Chew, Y. K., Tan, H. Y., Reuveny, S., & Weng Oh, S. K (2015). Increasing efficiency of human mesenchymal stromal cell culture by optimization of microcarrier concentration and design of medium feed. *Cytotherapy*, *17*(2), 163–173.

Chen, A. K.-L., Reuveny, S., & Oh, S. K. W. (2013). Application of human mesenchymal and pluripotent stem cell microcarrier cultures in cellular therapy: Achievements and future direction. *Biotechnology Advances*, *31*(7), 1032–1046.

Cherry, R. S., & Papoutsakis, E. T. (1986). Hydrodynamic effects on cells in agitated tissue culture reactors. *Bioprocess Engineering*, *1*, 29–41.

Cherry, R. S., & Papoutsakis, E. T. (1988). Physical mechanisms of cell damage in microcarrier cell culture bioreactors. *Biotechnology and Bioengineering*, *32*(8), 1001–1014.

Croughan, M. S. (1988). *Hydrodynamic effects on animal cells in microcarrier bioreactors* (Doctoral dissertation). Massachusetts Institute of Technology.

Croughan, M. S., Hamel, J.-F. P., & Wang, D. I. (1988). Effects of microcarrier concentration in animal cell culture. *Biotechnology and Bioengineering*, *32*, 975–982.

Dominici, M., LeBlanc, K., Mueller, I., Slaper-Cortenbach, I., Marini, F., Krause, D., Deans, R., Keating, A., Prockop, D., & Horwitz, E. (2006). Minimal criteria for defining multipotent mesenchymal stromal cells. the International Society for Cellular Therapy position statement. *Cytotherapy*, *8*, 315–317.

Engler, A. J., Sen, S., Sweeney, H. L., & Discher, D. E. (2006). Matrix elasticity directs stem cell lineage specification. *Cell*, *126*, 677–689.

Frank, V., Kaufmann, S., Wright, R., Horn, P., Yoshikawa, H. Y., Wuchter, P., Madsen, J., Lewis, A. L., Armes, S. P., Ho, A. D., & Tanaka, M. (2016). Frequent mechanical stress suppresses proliferation of mesenchymal stem cells from human bone marrow without loss of multipotency. *Scientific Reports*, *6*, 24264.

Godara, P., McFarland, C. D., & Nordon, R. E. (2008). Design of bioreactors for mesenchymal stem cell tissue engineering. *Journal of Chemical Technology & Biotechnology*, *83*, 408–420.

Hewitt, C. J., Lee, K., Nienow, A. W., Thomas, R. J., Smith, M., & Thomas, C. R. (2011). Expansion of human mesenchymal stem cells on microcarriers. *Biotechnology Letters*, *33*(11), 2325–2335.

Hoch, A. I., & Leach, J. K. (2014). Concise review: Optimizing expansion of bone marrow mesenchymal stem/stromal cells for clinical applications. *Stem Cells Translational Medicine*, *3*, 643–652.

Hu, W. S., Meier, J., & Wang, D. I. C. (1985). A mechanistic analysis of the inoculum requirement for the cultivation of mammalian cells on microcarriers. *Biotechnology and Bioengineering*, *27*, 585–595.

Huebsch, N., Arany, P. R., Mao, A. S., Shvartsman, D., Ali, O. A., Bencherif, S. A., Rivera-Feliciano, J., & Mooney, D. J. (2010). Harnessing traction-mediated manipulation of the cell/matrix interface to control stem-cell fate. *Nature Materials*, *9*, 518–526.

Ikebe, C., & Suzuki, K. (2014). Mesenchymal stem cells for regenerative therapy: Optimization of cell preparation protocols. *BioMed Research International*, *2014*, 951512.

Laner-Plamberger, S., Lener, T., Schmid, D., Streif, D. A., Salzer, T., Öller, M., Hauser-Kronberger, C., Fischer, T., Jacobs, V. R., Schallmoser, K., Gimona, M., & Rohde, E. (2015). Mechanical fibrinogen-depletion supports heparin-free mesenchymal stem cell propagation in human platelet lysate. *Journal of Translational Medicine*, *13*, 354.

Loubière, C., Sion, C., De Isla, N., Reppel, L., Guedon, E., Chevalot, I., & Olmos, E. (2019). Impact of the type of microcarrier and agitation modes on the expansion performances of mesenchymal stem cells derived from umbilical cord. *Biotechnology Progress*, *35*, e2887.

Maillot, C., Sion, C., De Isla, N., Toye, D., & Olmos, E. (2021). Quality by design to define critical process parameters for mesenchymal stem cell expansion. *Biotechnology Advances*, *50*, 107765.

Martin, C. (2017). *Étude des procédés daamplification de cellules souches mésenchymateuses humaines* (Doctoral dissertation). Universite de Lorraine.

McKee, C., & Chaudhry, G. R. (2017). Advances and challenges in stem cell culture. *Colloids and Surfaces B: Biointerfaces*, *159*, 62–77.

Mishra, R., Militky, J., Baheti, V., Huang, J., Kale, B., Venkataraman, M., Bele, V., Arumugam, V., Zhu, G., & Wang, Y. (2014). The production, characterization and applications of nanoparticles in the textile industry. *Textile Progress*, *46*, 133–226.

Öncül, A. A. (2010). *Simulation of interacting populations in inhomogeneous flows using reduced models* (Doctoral dissertation). Otto von Guericke University Library.

Parekkadan, B., & Milwid, J. M. (2010). Mesenchymal stem cells as therapeutics. *Annual Review of Biomedical Engineering*, *12*, 87–117.

Reppel, L. (2014). *Potentialité des cellules stromales de la gelée de Wharton en ingénierie du cartillage* (Doctoral dissertation). Universite de Lorraine.

Riazifar, M., Pone, E. J., Lötvall, J., & Zhao, W. (2017). Stem cell extracellular vesicles: Extended messages of regeneration. *Annual Review of Pharmacology and Toxicology*, *57*, 125–154.

Ringe, J., Kaps, C., Burmester, G.-R., & Sittinger, M. (2002). Stem cells for regenerative medicine: Advances in the engineering of tissues and organs. *Die Naturwissenschaften*, *89*(8), 338–351.

Rodriguez Fuentes, D. E., Fernández-Garza, L. E., Samia-Meza, J. A., Barrera-Barrera, S. A., Caplan, A. I., & Barrera-Saldaña, H. A. (2021). Mesenchymal stem cells current clinical applications: A systematic review. *Archives of Medical Research*, *52*, 93–101.

Romani, P., Valcarcel-Jimenez, L., Frezza, C., & Dupont, S. (2021). Crosstalk between mechanotransduction and metabolism. *Nature Reviews Molecular Cell Biology*, *22*, 22–38.

Russell, A. L., Lefavor, R. C., & Zubair, A. C. (2018). Characterization and cost-benefit analysis of automated bioreactor-expanded mesenchymal stem cells for clinical applications. *Transfusion*, *58*, 2374–2382.

Sion, C., Loubière, C., Wlodarczyk-Biegun, M. K., Davoudi, N., Muller-Renno, C., Guedon, E., Chevalot, I., & Olmos, E. (2020). Effects of microcarriers addition and mixing on WJ-MSC culture in bioreactors. *Biochemical Engineering Journal*, *157*, 107521.

Sion, C., Ghannoum, D., Ebel, B., Gallo, F., de Isla, N., Guedon, E., Chevalot, I., & Olmos, E. (2021). A new perfusion mode of culture for WJ-MSCs expansion in a stirred and online monitored bioreactor. *Biotechnology and Bioengineering*, *118*(11), 4453–4464.

Trounson, A., & McDonald, C. (2015). Stem cell therapies in clinical trials: Progress and challenges. *Cell Stem Cell*, *17*, 11–22.

Vining, K. H., & Mooney, D. J. (2017). Mechanical forces direct stem cell behaviour in development and regeneration. *Nature Reviews Molecular Cell Biology*, *18*, 728–742.

Zhu, A. J., Haase, I., & Watt, F. M. (1999). Signaling via β1 integrins and mitogen-activated protein kinase determines human epidermal stem cell fate in vitro. *Proceedings of the National Academy of Sciences of the United States of America*, *96*, 6728–6733.

Zwietering, T. (1958). Suspending of solid particles in liquid by agitators. *Chemical Engineering Science*, *8*, 244–253.

SUPPORTING INFORMATION

Additional supporting information can be found online in the Supporting Information section at the end of this article.

How to cite this article: Maillot, C., De Isla, N., Loubiere, C., Toye, D., & Olmos, E. (2022). Impact of microcarrier concentration on mesenchymal stem cell growth and death: Experiments and modeling. *Biotechnology and Bioengineering*, 119, 3537–3548. https://doi.org/10.1002/bit.28228